Scattering of polarized tritons by ^{9}Be and ^{12}C†

P. A. Schmelzbach,* R. A. Hardekopf, R. F. Haglund, Jr., and G. G. Ohlsen
Los Alamos Scientific Laboratory, University of California, Los Alamos, New Mexico 87545
(Received 9 May 1977)

The differential cross section and the analyzing power A_y for ^{9}Be$(\vec{t},t)^{9}$Be and ^{12}C$(\vec{t},t)^{12}$C elastic scattering have been measured at 15 and 17 MeV over the angular range $\theta_{lab} = 17.5$–$165.0°$. The data in the forward hemisphere have been analyzed with a standard optical model. A large depth and conventional geometry parameters for the spin-orbit potential have been found. The results of the present analysis are in general agreement with previous work involving polarized tritons scattered from heavy target nuclei and show important differences from investigations of the scattering of polarized helions on light nuclei.

[NUCLEAR REACTIONS ^{9}Be$(\vec{t},t)^{9}$Be, ^{12}C$(\vec{t},t)^{12}$C, $E=15,17$ MeV; measured $d\sigma/d\Omega(\theta)$, $A_y(\theta)$; deduced optical model parameters.]

I. INTRODUCTION

Past attempts to determine the parameters of the spin-orbit potential for mass-3 projectiles have had only limited success, owing primarily to the insensitivity of the differential cross section to these quantities and to the paucity of polarization data. The most extensive measurements of ^{3}He polarizations in elastic scattering were made by McEver *et al.*[1] using ^{9}Be, ^{12}C, and ^{16}O targets in a double-scattering experiment. These authors concluded that a spin-orbit potential at least 3 MeV deep was required to predict the observed polarizations. In contrast, theoretical estimates based on simplified assumptions[2,3] predicted the spin-orbit potential for mass-3 particles to be one-third as deep as for nucleons, or about 2 MeV.

Now that beams of polarized helions[4] and tritons[5] are available, one can expect systematic studies to shed new light on the spin dependence of the optical potential. One such study has recently been carried out by the Birmingham group, which investigated the scattering of 33 MeV polarized helions from ^{9}Be, ^{12}C (Ref. 6), ^{26}Mg, and ^{27}Al (Ref. 7). From the analysis of those data with a standard optical model, the authors concluded that the shape of the spin-orbit potential could be determined unambiguously. From the ^{9}Be and ^{12}C data a spin-orbit diffuseness parameter $a_{so} \approx 0.16$ was extracted. The radius was found to be slightly larger than the radius of the real potential. Although not given uniquely by that analysis, the spin-orbit strength was compatible with the folding-model predictions. In the ^{26}Mg and ^{27}Al case, both diffuseness ($a_{so} \approx 0.2$ fm) and radius were found to be significantly smaller than those of the real potential. V_{so} was well determined and a value of $V_{so} = 2.30$ MeV was selected. The failure of the folding model was attributed to the fact that the predicted potentials do not satisfy the above geometry criteria.

Hardekopf, Veeser, and Keaton[8] demonstrated that the folding model was not able to reproduce the analyzing powers observed in the scattering of 15-MeV polarized tritons by ^{52}Cr, ^{60}Ni, ^{90}Zr, ^{116}Sn, and ^{208}Pb. In a preliminary analysis of the data with a standard optical model, they obtained reasonable fits with geometry parameters for the spin-orbit potential close to those of the central potential. While a change of ±2 MeV in V_{so} could be nearly compensated by readjusting the depth of the imaginary potential, the best fits resulted for $V_{so} \geq 6$ MeV, indicating that the spin-orbit strength for tritons is about as large as for nucleons.

Since one would expect similar results for both mass-3 projectiles, the discrepancy between the results obtained is intriguing. The fact that deformed light nuclei may not be suitable for optical-model studies certainly can limit the generality of the helion-scattering results, but the differences between the two investigations cannot be attributed to such an effect without further investigation of both helion and triton scattering. It is therefore necessary to cover the same mass range with both projectiles. Since the presently available beams of polarized ^{3}He and tritons do not cover the same energy range, precise measurements at the same energy are presently not possible. However, a comparison of earlier measurements of the ^{12}C$(^{3}$He, $^{3}\vec{\text{H}}$e$)^{12}$C (Ref. 1) and ^{12}C$(t,\vec{t})^{12}$C (Ref. 9) scattering, both made with double-scattering apparatus at 18 MeV, shows that the polarization data agree almost point for point. Since the uncertainties in the two experiments are comparable and reasonably small in magnitude, the agreement between the two sets of data implies, *a priori*, that the spin-orbit potentials for ^{3}He and tritons

cannot be substantially different, at least at this energy.

It was the purpose of the present work to extend the Los Alamos investigation with polarized tritons to the light target nuclei ^{9}Be and ^{12}C for comparison with the polarized-helion results. Angular distributions of the analyzing power and the cross section were measured at triton energies of 15 and 17 MeV. In order to fulfill the requirements of more sophisticated future analyses, the angular range covered by the measurements was also extended to the backward direction.

II. EXPERIMENTAL METHOD

The beam was provided by the Los Alamos polarized triton source[5] and FN tandem Van de Graaff accelerator. Intensities up to 60 nA of about 80% polarized tritons were available at the target. Self-supporting targets of 1.9-mg cm^{-2} ^{12}C and 2-mg cm^{-2} ^{9}Be were mounted in a 60-cm cubical scattering chamber.[10] The detection system consisted of two pairs of counter telescopes 15° apart in the horizontal plane. The forward-angle pair was equipped with 150-μm ΔE and 1500-μm E surface-barrier silicon detectors. For the backward-angle pair the thicknesses were 50 and 1000 μm. By changing the lab angle in steps of 2.5°, the angular range between 17.5° and 165° could be covered, many points being measured twice. The angular resolution as defined by slits 3.33 mm wide and 11.4 mm high was ±0.4°. The detector position was set remotely by the on-line computer to an accuracy of ±0.02°. More details of the scattering chamber and the beam collimation are given in Ref. 10.

The ΔE and E signals were preamplified in two stages and after amplification sent to a mixer coder. Coincident ΔE-E pulses were forwarded with a routing pulse through analog-to-digitial converters to the on-line computer where mass identification was accomplished following the procedure described in Ref. 11. The peak-integration routine allowed for linear background subtraction. However, since in both experiments the spectra were of high quality, background subtraction was generally not necessary.

Measurements were performed at 15 and 17 MeV using the following method. With the counter telescopes set at equal angles left and right of the incident beam direction, runs of equal accumulated charge were taken for spin-up and spin-down directions (perpendicular to the scattering plane). The beam intensity was selected so as to reduce the dead time below 2% and the beam polarization was measured before and after each spin-up and spin-down run using the quench-ratio technique.[5,12]

The geometric mean method[13] was used to extract the cross section and analyzing power from the four integrated peak sums. This method eliminates all first-order errors in A_y associated with instrumental asymmetries and alignment errors. The analyzing power is given by

$$A_y = \frac{1}{p}\,\frac{L-R}{L+R}$$

and the unpolarized cross section σ_0 is proportional to

$$Y = L + R,$$

where L and R are the following geometric means of the integrated peak sums:

$$L = [(\text{left, spin up})\ (\text{right, spin down})]^{1/2},$$

$$R = [(\text{right, spin up})\ (\text{left, spin down})]^{1/2},$$

and p is the beam polarization. The uncertainty in the beam energy is estimated to be ±10 keV and the target half-thicknesses were about 70 keV.

III. EXPERIMENTAL RESULTS

Angular distributions of the analyzing power A_y and of the unpolarized differential cross section were measured for ^{9}Be and ^{12}C at triton lab energies of 15 and 17 MeV. The lab angular range between 17.5° and 165° was covered in steps of 2.5° for most of the data. For ^{12}C at 15 MeV a few measurements at intermediate angles were made around the strong negative peak of the angular distribution in the forward direction. The angular distributions are shown in Figs. 1–4. The data are available in tabular form from any of the authors.[14]

The statistical error of the analyzing power measurements is generally smaller than 0.01. The beam polarization was seen to be nearly constant during the course of the experiment, with differences between two successive polarization measurements generally smaller than 0.005. Hence, the contribution of polarization fluctuations to the relative error is smaller than 1%. The error due to other random uncertainties such as instability in the position of the beam is estimated to be less than 0.005.

The scale error due to the uncertainty in the absolute determination of the beam polarization from the quench-ratio method is estimated to be smaller than 2%.[5]

The relative error of the differential cross section measurement is mainly due to statistical errors and to the uncertainty arising from the setting of limits for the peak integration and background subtraction (when this was necessary). In some cases, there is an additional error due to

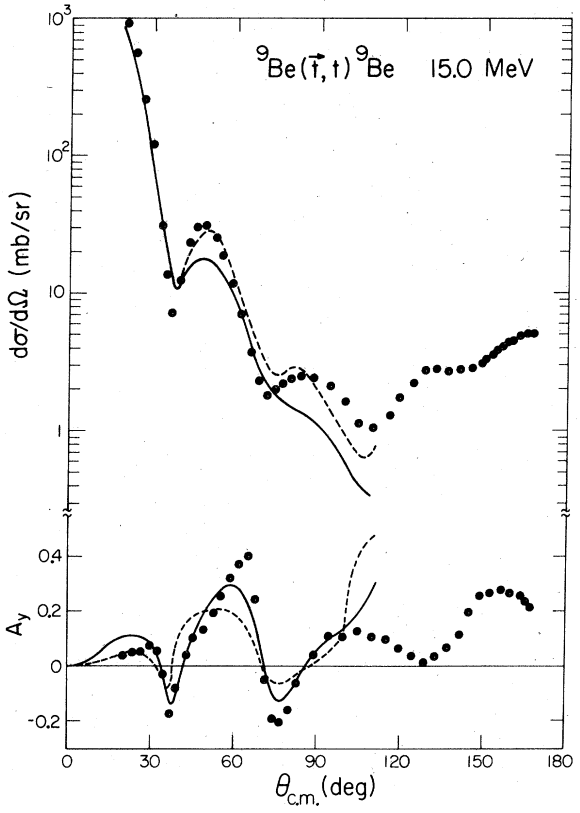

FIG. 1. The differential cross section and analyzing power for ^{9}Be($\vec{t}$,t)^{9}Be elastic scattering at 15.0 MeV. Relative errors are smaller than the plotting symbols. The solid and dashed curves are optical-model fits to the data, and are discussed in Sec. IV B 1.

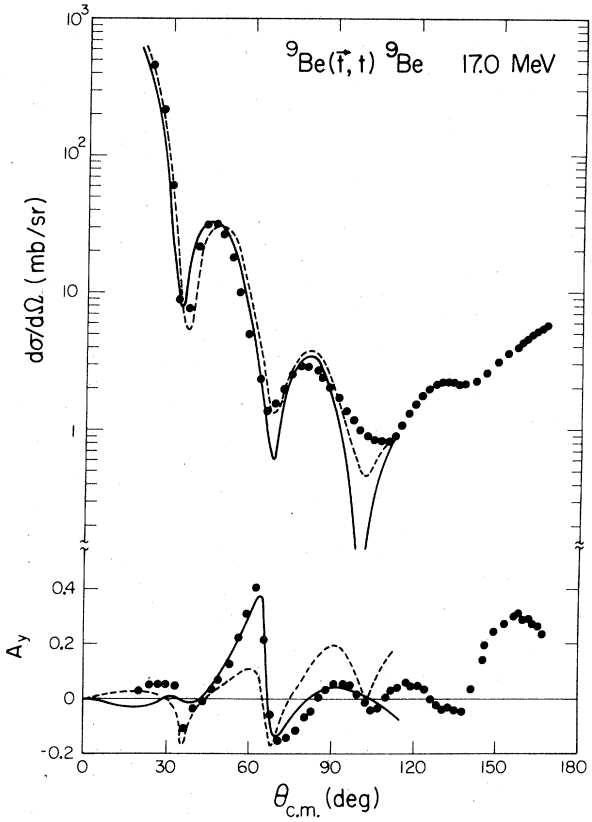

FIG. 2. The differential cross section and analyzing power for ^{9}Be($\vec{t}$,t)^{9}Be elastic scattering at 17.0 MeV. The relative errors in the data are smaller than the plotting symbols. The solid and dashed curves are optical-model fits to the data, and are discussed in Sec. IV B 2.

electronic cutoffs on the low energy side of the peaks which were overlooked during the experiment. Therefore, a relative error of 3% is assumed for the present cross section data.

Since no attempt to measure absolute cross sections was made in this experiment, the normalization was done in the following way: If one compares the present $t+^{12}$C measurements with the previous results of Keaton *et al.*[15] at 16 and 20 MeV, one sees that the maximum value of the cross section near 40° changes only slightly with energy. The present results were therefore normalized by interpolation to the results of Ref. 15. The accuracy of this normalization is not expected to be better than 10–15%.

A rough normalization for the $t+^9$Be measurements was obtained by comparing the thickness of the ^{9}Be and ^{12}C targets. The normalization obtained in this way was allowed to float during the optical-model analysis discussed in the next section. Since at both energies and for the potentials accepted the normalization factor converged to the same value, this value was used for the final calibration of the $t+^9$Be elastic cross section shown on Fig. 1. The uncertainty of this calibration is estimated to be ±15%.

Both ^{9}Be$+t$ and ^{12}C$+t$ scattering show very similar features in the forward hemisphere. The cross sections change only slightly between the two energies. The most difference is the appearance of a new structure at $\theta_{c.m.} = 60°$ for the ^{12}C($\vec{t}$, t)^{12}C scattering. The analyzing power for both scattering processes displays positive values at small angles, then a sharp negative peak followed by a broad positive part of the angular distribution which evolves with a strong slope into a negative minimum followed by a positive maximum. At larger angles both analyzing power and cross section become more energy-dependent, particularly A_y for ^{12}C($\vec{t}$, t)^{12}C. A noteworthy feature of the analyzing power for the $\vec{t}+^{12}$C scattering is the large values of A_y at several energy-angle combinations where it almost equals ±1.

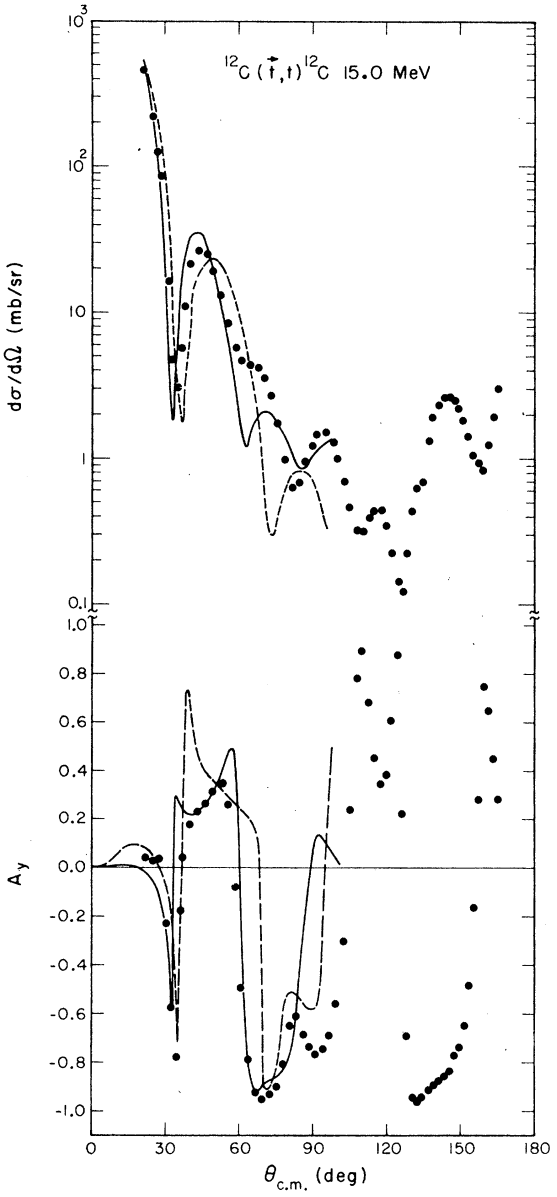

FIG. 3. The differential cross section and analyzing power for $^{12}C(\vec{t},t)^{12}C$ elastic scattering at 15.0 MeV. The relative errors are smaller than the plotting symbols. The optical-model calculations indicated by the smooth curves are discussed in Sec. IV B 3.

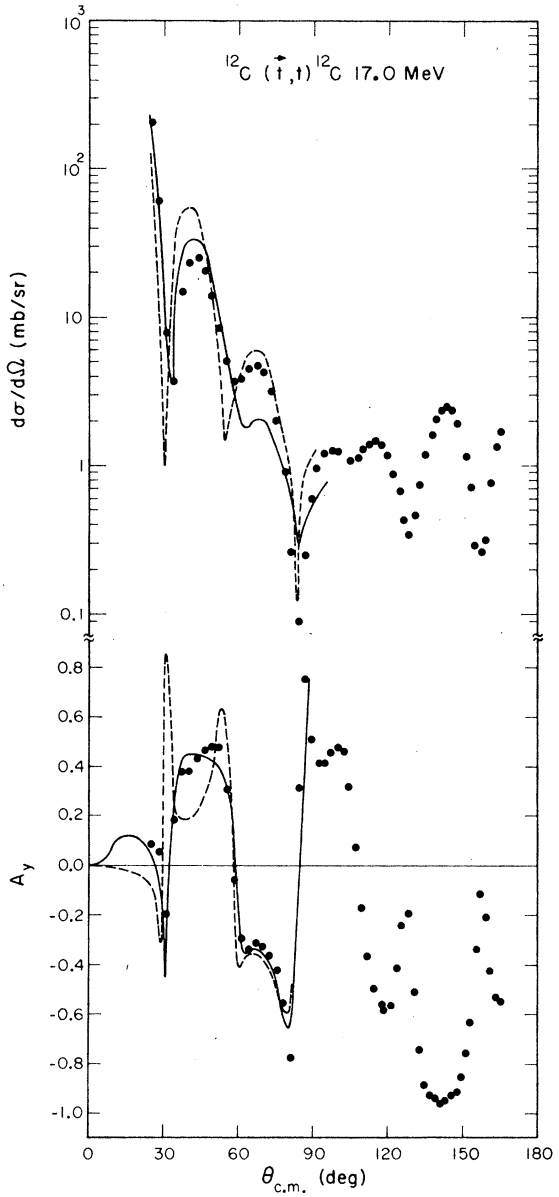

FIG. 4. The differential cross section and analyzing power for $^{12}C(\vec{t},t)^{12}C$ elastic scattering at 17.0 MeV. Relative errors are smaller than the plotting symbols. The optical-model fits indicated by the solid and dashed curves are discussed in Sec. IV B 4 of the text.

IV. OPTICAL-MODEL ANALYSIS

A. General description

From the measured energy dependence of both observables, it appears that a standard optical-model analysis would be successful in reproducing the data in the forward hemisphere only, where compound or multistep effects are believed to be less important than at backward angles.

The LASL version of Schwandt's optical-model code SNOOPY3 (Ref. 16) was used in this analysis. A charge radius $r_c = 1.3$ fm was used, and in order to reduce the number of free parameters and to escape the problem of the continuous depth-radius ambiguity, the radius r_0 of the real central potential was kept constant during the searches. In the first stage of the search different groups of two to four parameters were allowed to vary simultan-

eously. Near a local minimum of the error surface the number of free parameters was increased and for the final steps all parameters were searched on simultaneously. Starting from potentials found in the literature[15] or from reasonable approximations (for example—parameters of the helion potentials[1,6]) the fit to the cross section was improved first; then both observables were analyzed simultaneously. In this procedure it was necessary to increase the relative weight of the cross section and of parts of the angular distribution for the analyzing power according to which structure one wanted to reproduce best. Generally, the weighting of the cross section was chosen to get comparable contributions from both observables to the χ^2 or to force the search to give a satisfactory fit to the cross section too. Due to this procedure, the total χ^2 is not a convenient measure of the overall fit to the data and the selection of solutions has to be based on visual inspection also. Another difficulty arises from the fact that a minimum of the total χ^2 may correspond to the minimum of the χ^2 for one observable (generally the analyzing power) only. The χ^2 for the other observable may even have a local maximum at this solution. Therefore, the choice of a solution may be strongly dependent on the relative weighting of the observables.

This difficulty in fitting both observables simultaneously illustrates the well-known fact that the standard optical model is too crude a description for scattering on light nuclei. In particular, the imaginary potentials used are a poor description of the absorption. While both volume and surface absorption may give satisfactory fits when the cross section alone is fitted, both forms of the imaginary potential fail to give good reproduction of the cross section if both observables are fitted simultaneously. The surface absorption seems to be slightly preferred, especially in the $\vec{t}+{}^{12}$C case.

A few calculations were made using a combination of the two imaginary forms and were rejected since the parameters converged toward unphysical values. Due to the poor definition of the error surface, and the strong correlation between the parameters, the parameters found during the searches may depend strongly on the starting values and the technique used (selection of the parameters searched on simultaneously, weighting of the data, etc.). Therefore, no unique solution could be found and the parameters corresponding to a best fit for a particular case have a very limited meaning. However, by covering large parts of the parameter space one can strongly restrict the range of parameter values giving acceptable fits to the data.

The data analyzed cover the angular range up to $\theta_{\text{c.m.}} = 100°$ for the $\vec{t}+{}^{12}$C scattering and up to $\theta_{\text{c.m.}} = 110°$ in the $\vec{t}+{}^{9}$Be case.

For both nuclei, the analysis was first performed at the higher energy. The potentials giving satisfactory fits at 17 MeV were then used as starting values for the analysis of the 15-MeV data.

For the $\vec{t}+{}^{12}$C case, the radius of the real central potential was set at 1.2 fm, a value which has proven satisfactory in previous triton optical-potential work.[17] Investigations with other values of r_0 showed that, within reasonable limits, this parameter had little influence on the results of the analysis. In the $\vec{t}+{}^{9}$Be case, the value $r_0 = 1.3$ fm was found to give a better fit to the cross section. But here too, the conclusions about the spin-orbit potential are not substantially changed by other reasonable choices of r_0.

While some exploratory (and unsuccessful) searches were performed with real potential depths around 50 MeV for the $^{12}\text{C}(\vec{t}, t)^{12}\text{C}$ scattering at 17 MeV, the present analysis is limited to real potential depths around three times the nucleon-nucleus potential depth.

B. Results and discussion

1. $^{9}Be(\vec{t},t)^{9}Be$ at $E_t = 15$ MeV

Two fits to the cross section and the analyzing power for the $^{9}\text{Be}(\vec{t}, t)^{9}\text{Be}$ scattering at 15 MeV are shown in Fig. 1. The corresponding potentials are given in Table I. The fit with the potential *BA*15 (volume absorption) is indicated by the solid line. The fit to the cross section is rather poor, par-

TABLE I. Optical-model parameters for $^{9}\text{Be}(\vec{t}, t)^{9}\text{Be}$ scattering.

Energy (MeV)	Set	V	a_0	W_s	W_D	r_W	a_W	V_{so}	r_{so}	a_{so}
15.0	*BA*15	142.78	0.416	34.27		1.276	0.952	9.00	1.623	0.448
	*BB*15	137.95	0.542		22.00	1.517	0.614	7.00	1.517	0.563
17.0	*BA*17	139.66	0.826		39.87	1.772	0.405	12.29	1.605	0.436
	*BB*17	137.82	0.650		43.22	1.515	0.502	4.00	2.051	0.244

$r_c = 1.3$ fm; $r_0 = 1.3$ fm

ticularly beyond $\theta_{c.m.} = 70°$ where the second maximum of the cross section is not reproduced. The fit to the analyzing power is better. However, the maxima and minima are not reproduced closely. A slightly better fit to the polarization data between 45° and 60° may only be achieved by a potential with $V_{so} \approx 14$ MeV. In this case, the remaining parameters are very close to the set *BA*15. The influence on the cross section is very small, with a slight improvement of the quality of the fit around 45°. More than indicating the need for a very deep spin-orbit potential, this fact illustrates the lack of sensitivity of the data to V_{so} for values above 6 MeV.

The broken line corresponds to the parameter set *BB*15 (surface absorption). With this set, the fit to the cross section is definitely improved; however, the calculated analyzing power is not in good agreement with the data. For smaller V_{so}, the absolute values of the analyzing power become smaller; therefore, V_{so} may not be much smaller than given by *BB*15.

2. $^9Be(\vec{t},t)^9Be$ at $E_t = 17$ MeV

Two sets of parameters for the surface absorption potential found at this energy are given in Table I. The fits are shown in Fig. 2. The solid line corresponds to potential *BA*17, characterized by a rather large V_{so}. The fit to the cross section is good up to 100°, at which angle a strong negative peak is displayed by the calculation but not by the data. The analyzing power is well reproduced above 40°. Potentials reproducing the data at forward angles do not fit the maximum at 60°.

The broken line corresponds to potential *BB*17 of Table I. This potential has a shallower spin-orbit well ($V_{so} = 4.00$ MeV) with a small diffuseness ($a_{so} = 0.244$ fm). The fit to the cross section at larger angles is improved, but the analyzing power is not reproduced correctly. The overly large predicted values at 90° seem to characterize spin-orbit potentials with small diffuseness, whereas the too small value at 60° is found for all calculations using a small V_{so}.

Due to the similarity of the data analyzed at 15 and 17 MeV one would expect a high degree of consistency between the parameters found at both energies. This was only partially the case for the accepted parameter sets *BB*15 and *BA*17. The diffuseness parameters have quite different values in the two cases. The two sets illustrate a behavior frequently observed during the searches. As the diffuseness parameters moved away from about 0.6 ± 0.1 fm, two of them converged to higher (lower) values, generally quite close together, and the third one took on smaller (larger) values. On the other hand, the differences in the depths and diffuseness of the imaginary potential may be partially explained by a continuous W_D-a_W ambiguity.

Both the imaginary potential and the spin-orbit potential are peaked at a distance larger than the radius of the real central potential. A precise determination of V_{so} appears to be impossible in this case, mainly because of a strong correlation with the imaginary potential parameters which are themselves poorly defined. However, the following conclusions can be drawn from the analysis of the ^{9}Be$(\vec{t}, t)^9$Be data: (1) potentials with $V_{so} < 6$ MeV are unable to reproduce the analyzing powers, and (2) the searches performed with "small" spin-orbit geometry were unsuccessful.

3. $^{12}C(\vec{t},t)^{12}C$ at $E_t = 15$ MeV

The solid curves in Fig. 3 are calculations using the parameter set *CA*15 (Table II). This parameter set was obtained by increasing the weights for data near 45° and 60°, thus forcing the optical-model search code to fit these points. Evidently, the potential *CA*15 does not fit the data at 90° and beyond. The dotted curves show a fit obtained by overweighting the data near 80°, thus forcing the calculation to reproduce the oscillation at that point. However, this calculation fails to reproduce the angular distributions between 30° and

TABLE II. Optical-model parameters for ^{12}C$(\vec{t}, t)^{12}$C scattering.

Energy (MeV)	Set	V	a_0	W_s	W_D	r_W	a_W	V_{so}	r_{so}	a_{so}
15.0	*CA*15	128.50	0.713		9.07	1.297	0.944	7.03	1.000	0.516
17.0	*CA*17	132.59	0.640		12.61	1.371	0.784	11.08	1.470	0.621
	*CB*17	121.98	0.795		13.03	1.462	0.745	15.35	1.425	0.195

$r_c = 1.3$ fm; $r_0 = 1.2$ fm

70°, and optical-model parameters for it are therefore not listed in Table II. This bias in favor of the 60° polarization data leads to difficulties in fitting the cross section data. The appearance of a sharp dip, rather than a shoulder, in the cross section calculation around 60° is typical of the problem. However, if one does *not* bias the fit in this way, the predicted analyzing powers are too small and the calculated cross section does not reproduce the structure at 60°, either.

In particular, the value of r_{so} is sensitive to the relative weighting of the cross section and analyzing power. If the cross section data are accorded a greater relative weight, the value of r_{so} in parameter set *CA*15 is appropriate. But, if a better fit to the analyzing power is required, the value of r_{so} must be increased to approximately 1.6 fm.

4. $^{12}C(\vec{t},t)^{12}C$ at 17 MeV

Two fits with conventional spin-orbit geometry (solid line; set *CA*17 of Table II) and small spin-orbit geometry (broken line, Set *CB*17 of Table II) are shown in Fig. 4. It was necessary to bias the fit in favor of the data around 60° in order to reproduce this structure. The effect on the cross section is the same as previously discussed (Sec. IV B 3). The parameter set *CA*17 is characterized by a fairly large value of V_{so}. If the requirement of closely fitting the 60° structure of the analyzing power is relaxed, the fit to the data around 45° becomes much better and V_{so} reduces to values about 6 to 8 MeV. For searches with V_{so} forced to values smaller than 5 MeV the calculated analyzing power becomes too small around 45°.

The calculations with small spin-orbit geometry (broken line) require an even larger value for V_{so}. The strong positive peak at 30° may be suppressed by reducing the radius of the imaginary part of the potential to a small and probably unphysical value of 0.3 fm. Further investigations with shallow spin-orbit potentials ($V_{so} \approx 2$–3 MeV) were not able to reproduce the data around 45°. In calculations with small V_{so}, one sees peaks near 30° and 50°, separated by a valley whose minimum value approaches zero. The general shape of the curve is similar to the broken line in Fig. 4. Therefore, regardless of the choice of V_{so}, potentials with small spin-orbit geometry are not able to reproduce the $^{12}C(\vec{t}, t)^{12}C$ data in the energy and angular range investigated.

V. CONCLUSION

The elastic scattering of polarized tritons on ^{9}Be and ^{12}C has been experimentally investigated at 15 and 17 MeV for a large angular range. While only modest differences in the observables between the two energies are seen in the forward direction, the data at large angles show important changes between 15 and 17 MeV particularly in the $\vec{t} + ^{12}C$ case. Because of this strong energy dependence, and because compound-nucleus effects were not considered in our analysis, one expects the standard optical-model calculations to produce acceptable fits to the data only in the forward hemisphere. Hence, the optical-model parameter sets given in Tables I and II should be viewed as first approximations to the elastic-scattering potentials. In that sense, the present analysis has produced acceptable parametrizations of the data.

The extraction of the spin-orbit potential parameters is made extremely difficult by the strong correlation between the parameters of the spin-orbit and the central potentials. The absorption seems not to be accurately determined by our analysis. Since the extracted parameters depend strongly on the way the data are weighted in the analysis and since the error surface appears to be only poorly defined, no unique solution could be found. Nevertheless, from the trends observed in the optical-model analysis and from the parameter sets which fit the data satisfactorily at forward angles, we are led to the following conclusions about the triton spin-orbit potential:

(1) The radius is close to or 0.2–0.3 fm larger than the radius of the central potential, indicating a peaking of the spin-orbit potential slightly outside the nuclear surface.
(2) The diffuseness is close to or smaller than the diffuseness of the central potential, the lower limit being about 0.4 fm.
(3) The depth is larger than 5 MeV, an acceptable mean value being 8 MeV.

The numerous searches performed to find spin-orbit potentials with small V_{so} and/or a_{so} were unsuccessful.

These conclusions are in agreement with those of a previous study of triton elastic scattering from targets with $A \geq 52$ (Ref. 8), but disagree with a recently published analysis of polarized helion scattering from ^{9}Be and ^{12}C at higher energies.[6] Whether the different results obtained from triton and helion scattering arise from isospin effects or from the substantial difference in bombarding energies can possibly be ascertained by further study and experiment. One promising approach would be to compare results of polarized triton and polarized helion scattering from the same but heavier targets. The data of Ref. 8 and a more complete investigation of triton scattering from nuclei with $A \geq 40$, now being performed at Los Alamos, may serve as a beginning for such an investigation. Ideally, of course, the

availability of polarized mass-3 particle beams at the same energies would make possible a more adequate comparison of scattering and reactions induced by polarized helions and tritons.

The validity of the present analysis is limited by the use of light and deformed nuclei as targets. Moreover, the difficulties of simultaneously analyzing cross sections and analyzing powers may argue a cautious reading of the optical-model results. However, the general agreement between analyses with light and heavy target nuclei encourages the use of conventional spin-orbit geometry for the description of triton scattering. A precise determination of the depth of the spin-orbit potential, however, can only be reached through a systematic investigation with heavy target nuclei, where some of the difficulties encountered with light target nuclei are not present.

The authors wish to thank Judith Gursky for the preparation of the targets and Louis Morrison for his technical assistance with the polarized triton source.

---

†Work supported by the U. S. ERDA.

*Visiting Staff Member from Eidgenössische Technische Hochschule, Zürich, Switzerland.

[1]W. S. McEver, T. B. Clegg, J. M. Joyce, E. J. Ludwig, and R. L. Walter, Nucl. Phys. A178, 529 (1972).

[2]A. Y. Abul-Magd and M. El-Nadi, Prog. Theor. Phys. 35, 798 (1966).

[3]P. W. Keaton, Jr., E. Aufdembrink, and L. R. Veeser, Los Alamos Scientific Laboratory Report No. LA-4379-MS, 1970 (unpublished).

[4]W. E. Burcham, O. Karban, S. Oh, and W. B. Powell, Nucl. Instrum. Methods 116, 1 (1974).

[5]R. A. Hardekopf, G. G. Ohlsen, R. V. Poore, and N. Jarmie, Phys. Rev. C 13, 2127 (1976).

[6]W. E. Burcham, J. B. A. England, R. G. Harris, O. Karban, and S. Roman, Nucl. Phys. A246, 269 (1975).

[7]M. D. Cohler, N. M. Clarke, C. J. Webb, R. J. Griffiths, S. Roman, and O. Karban, J. Phys. G 2, L151 (1976).

[8]R. A. Hardekopf, L. R. Veeser, and P. W. Keaton, Jr., Phys. Rev. Lett. 35, 1623 (1975).

[9]D. D. Armstrong and P. W. Keaton, Los Alamos Scientific Laboratory Report No. LA-4538, 1970 (unpublished).

[10]P. A. Lovoi, Ph.D. thesis, Los Alamos Scientific Laboratory Report No. LA-6041-T, 1975 (unpublished); G. G. Ohlsen and P. A. Lovoi, in *Proceedings of the Fourth International Symposium on Polarization Phenomena in Nuclear Reactions*, edited by W. Grüebler and V. König (Birkhäuser, Basel, 1976), p. 907.

[11]D. D. Armstrong, J. G. Beery, E. R. Flynn, W. S. Hall, P. W. Keaton, Jr., and M. P. Kellogg, Nucl. Instrum. Methods 70, 69 (1969).

[12]G. G. Ohlsen, J. L. McKibben, G. P. Lawrence, P. W. Keaton, Jr., and D. D. Armstrong, Phys. Rev. Lett. 27, 599 (1971).

[13]G. G. Ohlsen and P. W. Keaton, Jr., Nucl. Instrum. Methods 109, 41 (1973).

[14]P. A. Schmelzbach, R. A. Hardekopf, R. F. Haglund, Jr., and G. G. Ohlsen, Los Alamos Scientific Laboratory Report No. LA-6791-MS, 1977 (unpublished).

[15]P. W. Keaton, Jr., D. D. Armstrong, L. R. Veeser, H. T. Fortune, and N. R. Roberson, Nucl. Phys. A179, 561 (1972).

[16]P. Schwandt, Indiana University, Code SNOOPY3, version 1971 (unpublished).

[17]F. D. Becchetti and G. W. Greenlees, in *Proceedings of the Third International Symposium on Polarization Phenomena in Nuclear Reactions*, edited by H. H. Barschall and W. Haeberli (Univ. of Wisconsin Press, Madison, 1970), p. 682.